Available online at www.sciencedirect.com
ScienceDirect
Journal of Power Sources 173 (2007) 688–694
JOURNAL OF POWER SOURCES
www.elsevier.com/locate/jpowsour

Raman scattering, DSC, XRD and ferroelastic domain studies at superionic phase transitions in $[(NH_4)_{1-x}Rb_x]_3H(SO_4)_2$ for $x > 0.8$

J. Wolak [a,*], M. Połomska [a], L. Szcześniak [a], A. Pietraszko [b], L.F. Kirpichnikova [c]

[a] *Institute of Molecular Physics, Polish Academy of Sciences, Poznań, Poland*
[b] *Institute of Low Temperatures and Structural Researches, Polish Academy of Sciences, Wrocław, Poland*
[c] *Institute of Crystallography, Russian Academy of Sciences, Moscow, Russia*

Available online 26 May 2007

Abstract

Ferroelastic domains, Raman scattering, XRD and DSC studies of $[(NH_4)_{0.14}Rb_{0.86}]_3H(SO_4)_2$ and $[(NH_4)_{0.1}Rb_{0.9}]_3H(SO_4)_2$ mixed crystals are presented. Two endothermic peaks were found for both crystals in DSC heating runs at T_S and T'_S. A difference $T'_S - T_S$ decreases with increasing Rb content. It was confirmed from X-ray diffraction studies that at T_S the crystal structure changes from $C2/c$ to $R\bar{3}m$. At T'_S the crystals undergo a successive structural transition to the phase which could be characterized by three dimensional system of virtual hydrogen bonds and a new type of virtual dimers. Our provisional XRD studies showed that the crystal structure at $T > T'_S$ may belongs to orthorhombic system. In Raman studies it was found that at T'_S the Raman spectra of $[(NH_4)_{0.1}Rb_{0.9}]_3H(SO_4)_2$ undergo conspicuous changes. All our studies revealed that the crystals become polycrystalline at T'_S, and temperature lowering results in a huge thermal hysteresis. It is presumed that structural relaxation exists in the crystals.

Keywords: Tri(ammonium/rubidium) hydrogen bisulfate; Superionic phase transitions; Ferroelastic domains; DSC; XRD; Raman scattering

1. Introduction

Solid acids, like those belonging to a family with general formula $M_xH_y(XO_4)_{(x+y)/2}$, where M = Rb, NH_4, Cs, K; X = S, Se, are characterized by the fact that XO_4 groups bound by hydrogen bonds form, either chains, dimers or trimers specifically ordered in the structure, depending on the crystal groups (e.g. different x and y). All members of the family undergo phase transitions to superionic phase, which is characterized by high proton conductivity. On passing through the transition conductivity jumps by several orders of magnitude to the value of 10^{-2} to $10^{-3}\ \Omega^{-1}\,cm^{-1}$ [1–5]. Therefore the crystals are very thoroughly studied in view of their possible application to fuel cells. For fuel cells application they offer the advantage of anhydrous proton transport and high temperature stability (up to 250 °C). Haile et al. [6] constructed a cell made of a $CsHSO_4$ electrolyte membrane (about 1.5 mm thick), operating at 150–160 °C in H_2/O_2 configuration. Such fuel cell exhibited promising electrochemical behavior.

In spite of the fact that the crystals have attracted the attention of researchers for a number of years, there still seem to be a lot of doubts connected with their properties.

$[(NH_4)_{1-x}Rb_x]_3H(SO_4)_2$ is a representative of an extremely interesting group of crystals which belong to $M_xH_y(XO_4)_{(x+y)/2}$ family with $x = 3$ and $y = 1$. All members of the group undergo a phase transition to superionic state with high proton conductivity [1–3]. For many members of the family, the transition to superprotonic phase at $T = T_S$ is simultaneously a ferroelastic–paraelastic one. The properties of pure components of $[(NH_4)_{1-x}Rb_x]_3H(SO_4)_2$, e.g. $(NH_4)_3H(SO_4)_2$ and $Rb_3H(SO_4)_2$ are completely different. $(NH_4)_3H(SO_4)_2$ exhibits a sequence of consecutive structural phase transitions—at $T_S \cong 415$ K a transition from superprotonic/paraelastic phase ($R\bar{3}m$-phase I) to the first ferroelastic state ($C2/c$-phase II) [7,8]. At $T_1 \cong 265$ K the crystal undergoes a phase transition from ferroelastic I to ferroelastic state II ($P2/n$) (phase III). At $T_2 \cong 145$ K the crystal undergoes an equistructural phase transition $P2/n \rightarrow P2/n$ (phase IV). At $T_3 \cong 135$ K a transformation from monoclinic $P2/n$ symmetry to triclinic $P\bar{1}$ (phase V) one takes place [9,10]. According to Gesi [11] high pressure induces ferroelectricity in $(NH_4)_3H(SO_4)_2$. High hydrostatic pressure applied to the crystal causes a fall in the temperature of superprotonic phase transition [8]. As opposed to

* Corresponding author.
E-mail address: wolak@ifmpan.poznan.pl (J. Wolak).

0378-7753/$ – see front matter © 2007 Elsevier B.V. All rights reserved.
doi:10.1016/j.jpowsour.2007.05.083

$(NH_4)_3H(SO_4)_2$, $Rb_3H(SO_4)_2$ undergoes only one phase transition from the monoclinic $C2/c$ phase to superprotonic one at $T_S \cong 490$ K and it does not exhibit ferroelastic properties below T_S [12,13]. Substitution of hydrogen by deuterium in $Rb_3H(SO_4)_2$ induces antiferroelectric properties below ~40 K [14]. Studying of $[(NH_4)_{1-x}Rb_x]_3H(SO_4)_2$ Baranov et al. [15] showed that for the concentration of Rb higher than 60% a new superionic phase transition to phase I′ appears at higher temperatures (above superionic phase I). The temperature of phase transition T_S' to a new phase I′ decreased with higher Rb content. Only phase I′ is observed in $Rb_3H(SO_4)_2$. Increased Rb content in $[(NH_4)_{1-x}Rb_x]_3H(SO_4)_2$ results in increased temperature of the ferroelastic–superionic phase transition T_S.

The studies of XRD, DSC, Raman scattering and ferroelastic domains behavior at two superionic phase transitions in the samples of $[(NH_4)_{1-x}Rb_x]_3H(SO_4)_2$ with $x > 0.8$ were the aim of our research. Studying the crystals of high Rb content we also wanted to understand the properties of the $Rb_3H(SO_4)_2$ crystal, so much different from the properties of other crystals—the representatives of the $M_3H(XO_4)_2$ family.

2. Experimental

$[(NH_4)_{1-x}Rb_x]_3H(SO_4)_2$ single crystals of pseudo-hexagonal habitus with well developed (0 0 1) plane were grown by slow evaporation of stoichiometric aqueous solution at room temperature.

Differential scanning calorimetric measurements were performed using Netzsch DSC 200 calorimeter both by heating and cooling single crystal samples from room temperature up to 510 K.

FT NIR Raman spectra were recorded using Bruker IFS66FRA106 spectrometer. The samples were excited with a 1064 nm diode-pumped Nd:YAG laser of output power ~150 mW. The samples of $[(NH_4)_{1-x}Rb_x]_3H(SO_4)_2$ were prepared in the form of thin square plates with the main surface perpendicular to the monoclinic c*-axis. Raman studies were carried out at 180° geometry. Deconvolution of the Raman peaks was carried out by the Levenberg–Marquardt method.

Ferroelastic domain structure along the c*-axis was observed in JENAPOL polarizing microscope.

Temperature studies, both Raman and in optical microscope, were carried out using Linkam cooling–heating stage.

Single-crystal X-ray studies were performed with KUMA KM4CCD diffractometer with graphite-monochromated Mo Kα radiation.

3. Results and discussion

3.1. Differential scanning calorimetry (DSC) studies

DSC studies of $[(NH_4)_{0.14}Rb_{0.86}]_3H(SO_4)_2$ and $[(NH_4)_{0.1}Rb_{0.9}]_3H(SO_4)_2$ revealed two high temperature thermal anomalies. Fig. 1 presents DSC runs on cooling and heating for $[(NH_4)_{0.14}Rb_{0.86}]_3H(SO_4)_2$, $[(NH_4)_{0.1}Rb_{0.9}]_3H(SO_4)_2$ together with those of $Rb_3H(SO_4)_2$. For the $[(NH_4)_{0.14}Rb_{0.86}]_3H(SO_4)_2$ single crystal (Fig. 1a) the first anomaly at $T_S \approx 473$ K

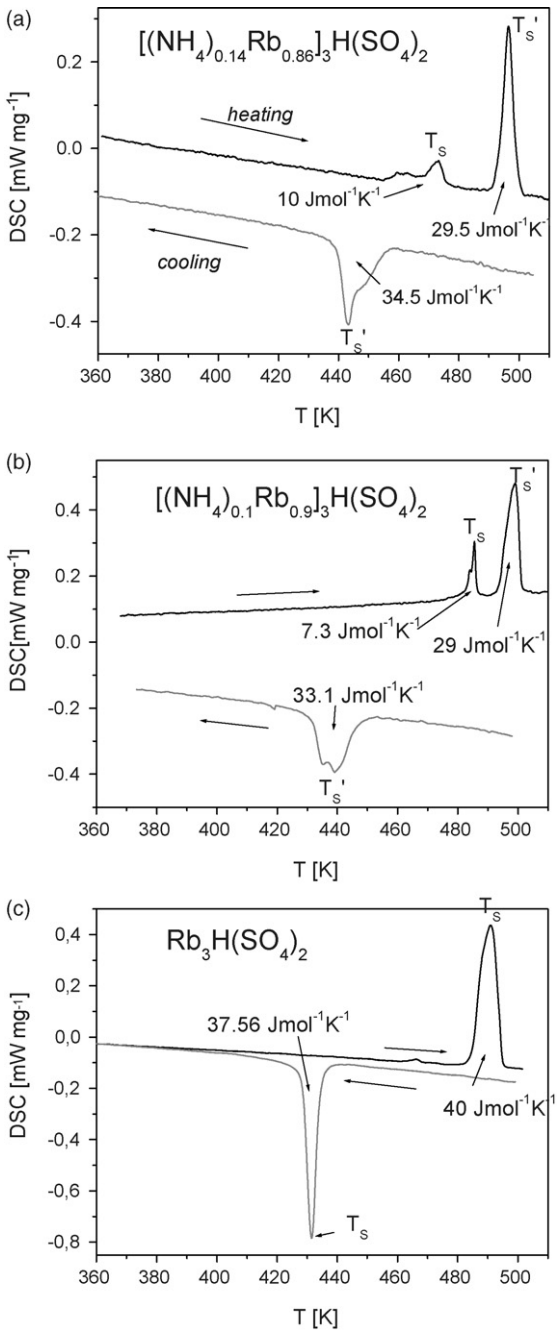

Fig. 1. DSC runs of $[(NH_4)_{0.14}Rb_{0.86})]_3H(SO_4)_2$ (a), $[(NH_4)_{0.1}Rb_{0.9})]_3H(SO_4)_2$ (b) and $Rb_3H(SO_4)_2$ (c) single crystals; the rates of heating and cooling were: 3 K min^{-1} (a); 3 K min^{-1} (b); 5 K min^{-1} (c).

with an enthalpy $\Delta H \cong 10.5$ J g^{-1} ($\Delta S = 10$ J mol^{-1} K^{-1}) is related to the ferroelastic (phaseII)–superprotonic (phaseI) phase transition. The second anomaly at $T_S' \approx 496$ K gives a significant change of enthalpy $\Delta H \cong 32.5$ J g^{-1}. ($\Delta S = 29.5$ J mol^{-1} K^{-1}) and is related to a phase transition to the second superionic phase (phase I′). On cooling in DSC run we could observe only one, small structurized thermal anomaly with enthalpy change of $\Delta H \cong -34$ J g^{-1} ($\Delta S = 34.5$ J mol^{-1} K^{-1}). The anomaly appeared at T = ~443 K. A huge thermal hysteresis could be related to high structural disorder which appears above T_S'. This thermal hysteresis may be explained as follows:

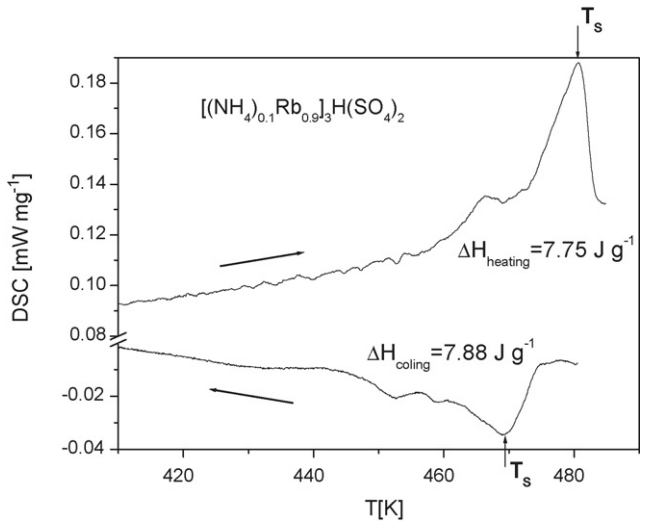

Fig. 2. DSC runs of $[(NH_4)_{0.1}Rb_{0.9})]_3H(SO_4)_2$ heated to $T_S < T < T'_S$; the rate of cooling and heating was 4 K min^{-1}.

after cooling the crystal needs time to recover to its low temperature structure, which means the ordering of protons in the dimer as well as the ordering of the dimers themselves. Similar behavior was already observed in $Rb_3H(SO_4)_2$ single crystals [16]. However, when the crystals with high Rb content are heated only to T_S, we do not observe a huge thermal hysteresis. Fig. 2 presents DSC runs for $[(NH_4)_{0.1}Rb_{0.9}]_3H(SO_4)_2$ crystal heated to $T_S < T < T'_S$. The phase transition is reversible with small temperature hysteresis $\Delta T_S \cong 8$ K. As one can see, the enthalpy for phase transition at T_S is nearly the same at heating and cooling runs. Our DSC studies revealed that during the first heating of the crystal "as grown" in all crystals studied T_S and T'_S are higher than those for consecutive heating runs.

3.2. Crystal structure

As an example of mixed crystals, we would like to present the results of X-ray studies of $[(NH_4)_{0.14}Rb_{0.86}]_3H(SO_4)_2$ single crystal. The temperature crystallographic data were collected in the temperature range from 295 to 520 K at 298, 445, 482 and 510 K. At room temperature the monoclinic $C2/c$ lattice parameters are the following $a = 15.2403(24)$ Å, $b = 5.8926(17)$ Å, $c = 10.1597(21)$ Å, $\beta = 102.401(11)^\circ$. In Fig. 3 the temperature dependence of the lattice parameters for $[(NH_4)_{0.14}Rb_{0.86}]_3H(SO_4)_2$ crystals is showed. The anomaly of lattice parameters indicates that this crystal undergoes structural phase transitions at $T_S \approx 473$ K and at $T'_S \approx 497$ K. The redetermination of the crystal structures confirms that the symmetry of the structures belongs to a monoclinic system with $C2/c$ at 455 K, to trigonal system with $R\bar{3}m$ at 482 K and to orthorhombic system at 510 K. During the transformation at T'_S the sample becomes polycrystalline, and there is some trouble with determining its crystal structure. Our first attempt to find the crystal structure in phase I′ were made using the powder X-ray method. The X-ray powder-diagram at 510 K is very similar to the diagram of the Rb_2SO_4 crystals, which belong to an orthorhombic system with *Pnma* space group in high temperature phase. The full determination of the crystal structure in phase I′ will be done in the near future. The projection of the crystal structure for $[(NH_4)_{0.14}Rb_{0.86}]_3H(SO_4)_2$, determined in the low-temperature phase at $T = 295$ K and in the phase above T_S at $T = 482$ K, is presented in Fig. 4A and B, respectively. Isolated dimers of $O_3SO\cdots H\text{-}OSO_3$, characteristic of the monoclinic phase, can be seen in Fig. 4A. In the trigonal phase I ($R\bar{3}m$), characterized by fast proton diffusion, the SO_4 groups are coupled by a two dimensional system of hydrogen bonds. The increase of displacement factor related to the thermal vibrations of oxygen atoms was observed at high temperature range $T_S < T < T'_S$ (see Fig. 4B).

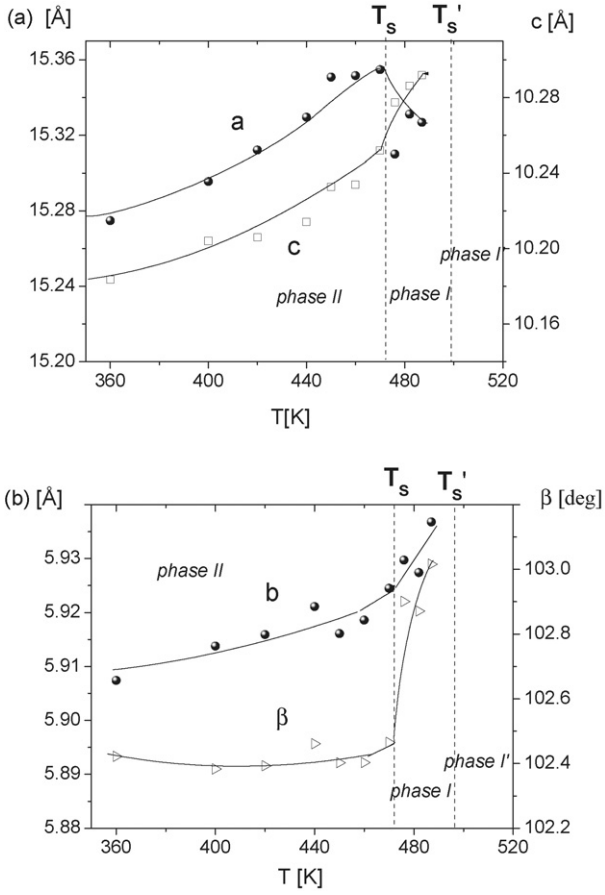

Fig. 3. Temperature dependences of lattice parameters of $[(NH_4)_{0.14}Rb_{0.86})]_3H(SO_4)_2$. The lines are guide for the eyes.

3.3. Ferroelastic domain structure

As it was already mentioned, $(NH_4)_3H(SO_4)_2$ exhibits ferroelastic properties below T_S. The mixed crystals with a high concentration of Rb are also ferroelastic below T_S. However their thermal evolution in the vicinity of the ferroelastic–paraelastic/superprotonic phase transition is quite different from that of the crystals with low Rb concentration [17,18]. Fig. 5 presents a sequence of ferroelastic domain patterns for $[(NH_4)_{0.1}Rb_{0.9}]_3H(SO_4)_2$ single crystal at different temperatures. The observations were carried out on the plane perpendicular to the monoclinic c*-axis. At room temperature

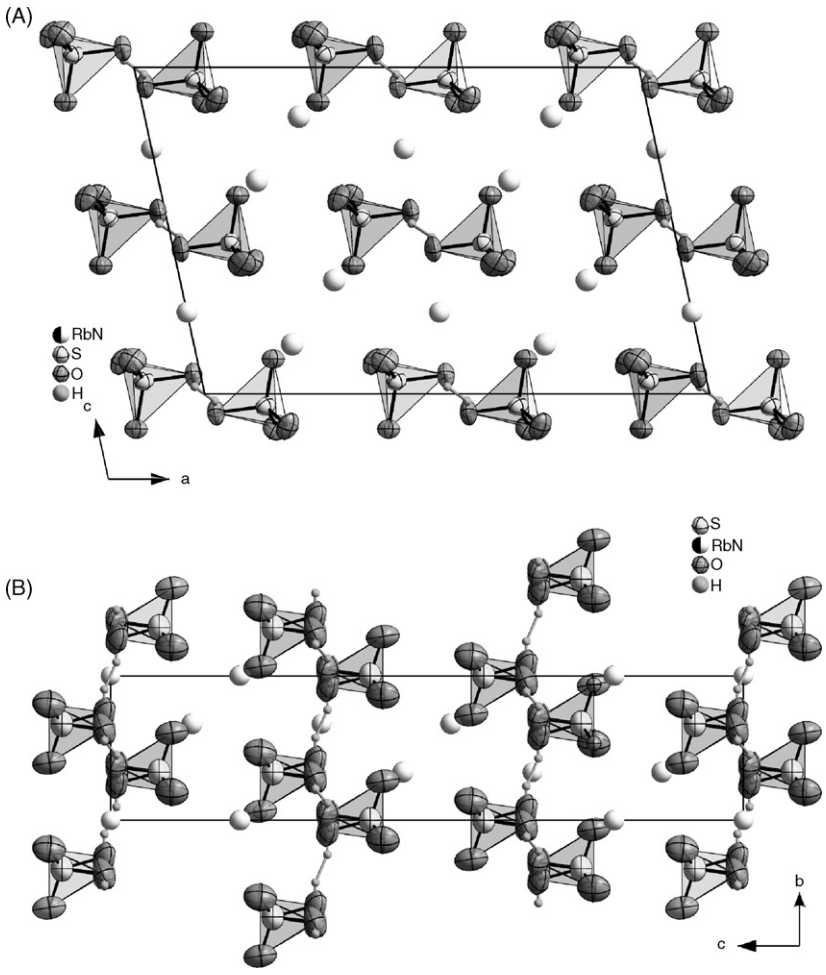

Fig. 4. Crystal structure of $[(NH_4)_{0.14}Rb_{0.86})]_3H(SO_4)_2$ at $T = 295$ K (A) and $T = 482$ K (B).

the crystal is in a single domain state. When the temperature increases at $T \approx T_S - 20$ K (Fig. 5b) ferroelastic domains appear in the crystal. The orientation of ferroelastic domain walls corresponds to a transformation from trigonal prototype symmetry $\bar{3}m$ to monoclinic $2/m$ one, according to Sapriel [19]. Further approach to the temperature of phase transition brings about a fragmentation (size reduction) of the domains (Fig. 5c) and their disappearance at $T = T_S \approx 488$ K (Fig. 5d). Further increase in temperature up to $T_S < T < T'_S$ results in the appearance of areas of different orientations (blocks) (Fig. 5e). If the temperature is lowered from $T_S < T < T'_S$, below T_S the crystal splits into very fine domains and remains in such a state up to room temperature (Fig. 5f–h). At T'_S the crystal passes to polycrystalline state, becomes opaque and stays in such a state down to room temperature.

3.4. Raman scattering studies

The structure of the crystals which belong to the $M_3H(XO_4)_2$ family, is characterized by the existence of isolated dimers at room temperature (see Fig. 4A), where a proton joins two SO_4 groups by means of a hydrogen bond. The ordering of protons in the dimer and the ordering of the dimers determine the properties of the crystals of that family. As it was mentioned before, at $T > T_S$ the crystals of the group exhibit high proton conductivity. The proton conductivity in high temperature phase can be imagined as near barrierless proton transfer between two oxygen atoms of the neighboring SO_4 tetrahedra and subsequent reorganization of proton environment. Such proton transfer can be described by Grotthus mechanism [20]. Therefore being familiar with temperature changes in the dynamics of the molecular groups forming the dimer is essential for studying phase transitions present in those crystals. Thus Raman scattering temperature studies enable us to investigate the role played by the components of $O_3SO\cdots H\text{-}OSO_3$ dimer in the mechanism of phase transition as well as the role of their dynamics in the mechanism of proton transport. As it was already mentioned, the $[(NH_4)_{1-x}Rb_x]_3H(SO_4)_2$ with $x > 0.8$ undergo two superionic phase transitions at T_S and T'_S. At both temperatures proton conductivity undergoes significant jumps, each about several orders of magnitude [15]. Fig. 6 presents temperature evolution of the Raman spectra of the $[(NH_4)_{0.1}Rb_{0.9}]_3H(SO_4)_2$ single crystal in the range corresponding to the internal vibration of the SO_4 tetrahedron. In the low conducting phase II the bands in the range between 300 and 700 cm^{-1} are assigned to doubly degenerated ν_2 and triply degenerated ν_4 bending vibrations of SO_4. The line at $\sim$960 cm^{-1} is related to the stretching νHOS vibration of HSO_4 entity, the line at $\sim$1060 cm^{-1} corresponds to

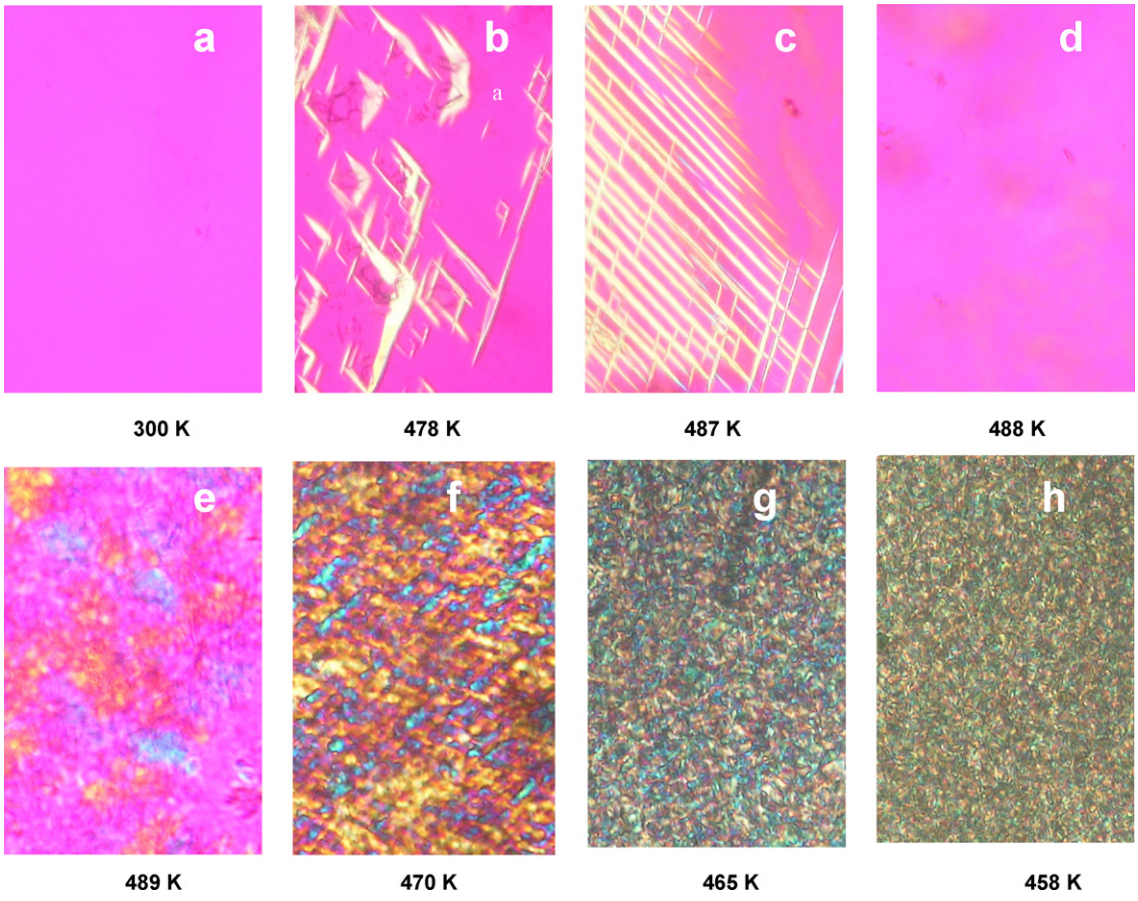

Fig. 5. Temperature evolution of ferroelastic domain patterns of $[(NH_4)_{0.1}Rb_{0.9})]_3H(SO_4)_2$.

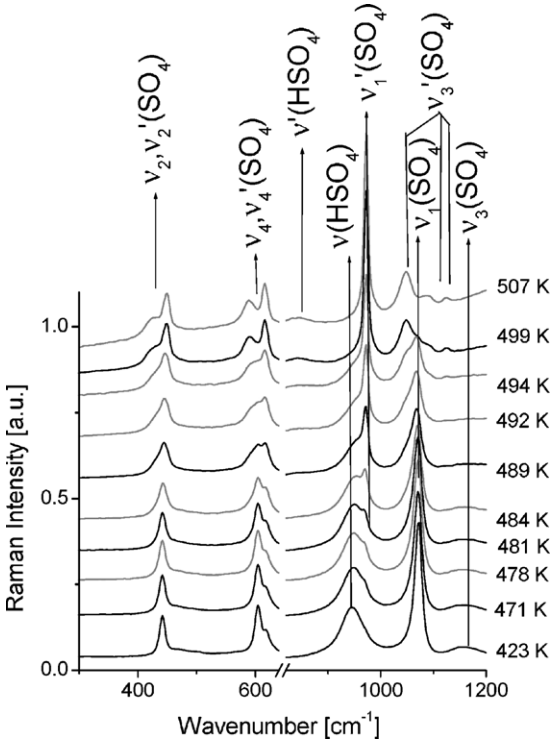

Fig. 6. Raman spectra as temperature dependent for $[(NH_4)_{0.1}Rb_{0.9})]_3H(SO_4)_2$ in the range of internal vibrations of SO_4 tetrahedron.

the symmetrical vibration νOS of ν_1SO_4 and a very broad band at $\sim$1190 cm^{-1} is related to a triply degenerated ν_3 stretching vibration [13,18].

At T_S' when the crystal transforms to a new superprotonic phase I′ the Raman spectrum of the $[(NH_4)_{0.1}Rb_{0.9}]_3H(SO_4)_2$ undergoes conspicuous changes. The lines at $\sim$1064 and $\sim$960 cm^{-1} assigned, respectively, to $\nu_1(SO_4)$ and $\nu(HSO_4)$ stretching vibrations in phases II and I, disappear. Also the band assigned to the $\nu_3(SO_4)$ stretching vibration, which is very broad in phases II and I, disappears in the phase I′. In phase I′ we can observe a very sharp, narrow line at $\sim$980 cm^{-1}, which we tentatively assigned to the $\nu_1'(SO_4)$ vibration. The new very broad line which appears at $\sim$820 cm^{-1} could be tentatively assigned to the stretching vibration of ν'HOS (= $\nu'HSO_4$). Very detailed temperature studies of the Raman spectra allowed us to create graphs (Figs. 7 and 8) which show temperature changes of the Raman lines connected with the stretching vibration of the SO_4 tetrahedra, discussed earlies, being a component of the dimers in all phases (I′, I and II). The anomaly, which appears at $T = T_S$, is characterized by a small jump like decreasing of $\nu_1(SO_4)$ and a conspicuous increase of $\nu_1'(SO_4)$ below T_S'. The $\nu_1'(SO_4)$ is nearly constant above T_S' (Fig. 7). The frequency $\nu(HSO_4)$ increases in the vicinity of T_S (Fig. 8). At $T > T_S'$, $\nu'(HSO_4)$ is nearly stable but is determined with small accuracy because of its small intensity and broadness. The changes observed in the range of the bending vibration $\nu_2(SO_4)$ and ν_4 (SO_4) are less

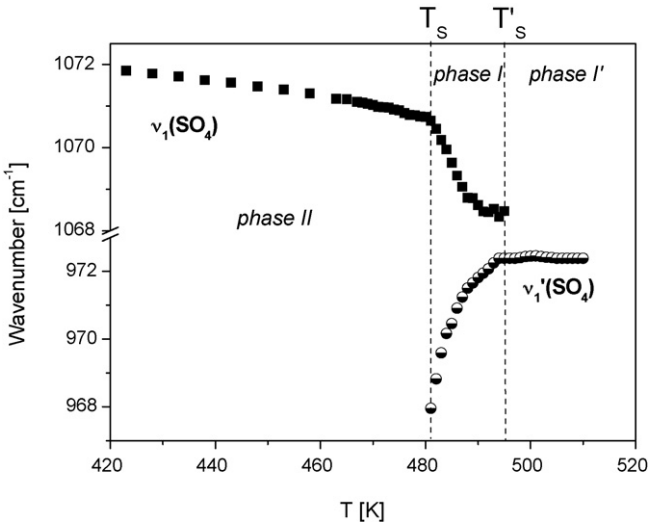

Fig. 7. Temperature dependence of ν_1 and ν_1' stretching vibration of SO_4 tetrahedron for $[(NH_4)_{0.1}Rb_{0.9})]_3H(SO_4)_2$.

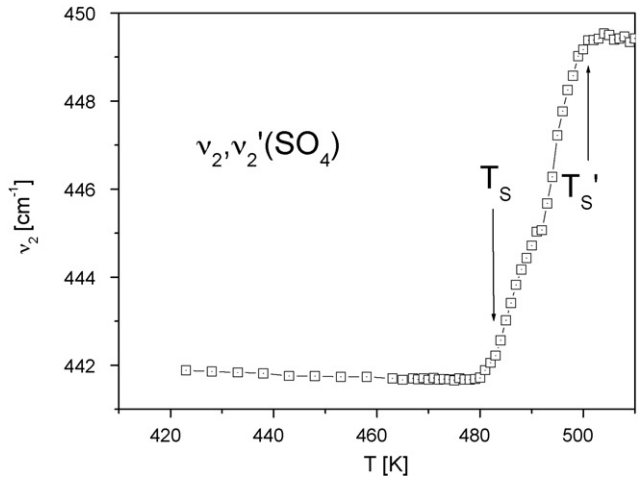

Fig. 9. Temperature dependence of ν_2 bending vibration of SO_4 tetrahedron for $[(NH_4)_{0.1}Rb_{0.9})]_3H(SO_4)_2$.

conspicuous. One component of a doubly degenerated vibration ν_2 at ~442 cm^{-1} changes with temperature as it is shown in Fig. 9. At T_S a rapid increase into higher wavenumbers is observed, and consecutive rapid increase in the band position is observed below T_S'. Above T_S' the Raman band position practically does not change. Additionally, at T_S', the second component of ν_2 appears at ~420 cm^{-1}. In the case of triply degenerated ν_4 bending vibration the Raman band intensity of one component at ~615 cm^{-1} increases with rising temperature, whereas the component at ~604 cm^{-1} disappears at T_S' and simultaneously a new component of ν_4 appears.

The comparison of the Raman spectra in the temperature range from 440 to 520 K for single crystal of $[(NH_4)_{0.1}Rb_{0.9}]_3H(SO_4)_2$ indicates that the arrangement of dimers of $O_3SO\cdots H\text{-}OSO_3$ in the new phase I′ is quite different from that below T_S'. The preliminary analysis of the crystal structure of phase I′ suggests that the SO_4 groups are strongly disordered and protons occupy statistically new positions forming the virtual hydrogen bonds between all oxygen atoms. The hydrogen bonds are longer than in the trigonal phase. We suppose that a three-dimensional system of virtual hydrogen bonds and a new type of virtual dimers exist in phase I′. New high temperature dimers (at $T > T_S'$) are characterized by stretching vibrations $\nu_1'(SO_4)$ at ~970 cm^{-1} and $\nu'(HSO_4)$ at ~820 cm^{-1}. Lowering the temperature of the crystal from $T > T_S'$, we can observe the existence of high-temperature phase to the temperatures much below T_S. Fig. 10 presents the Raman spectra of the studied crystal measured at room temperature 1 day after temperature studies. The spectra of "as grown" crystal and in high temperature phase (at $T > T_S'$), were presented to facilitate comparison making. As we can see, the spectrum of the crystal which was in the high-temperature phase at temperatures $T > T_S'$ contains both bands of the low- and high-temperature phases. Moreover, we can notice there some bands (at ~891, 995 and 1019 cm^{-1}) which are not present in any of these phases. We suspect that the crystal needs quite a considerable amount of time to pass from the state characterized by high structural disorder to

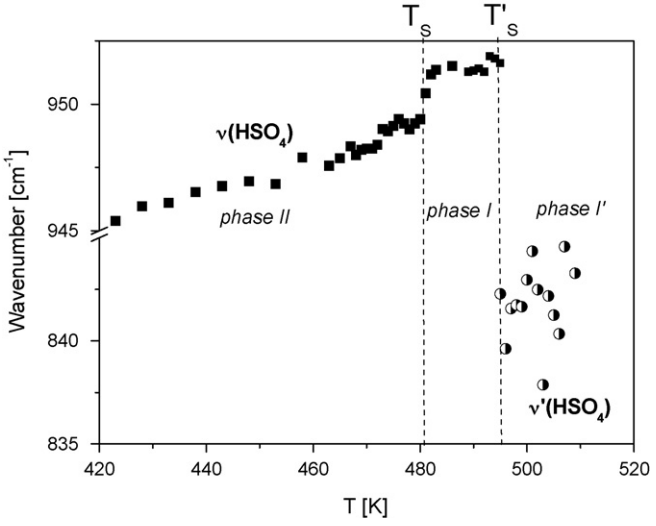

Fig. 8. Temperature dependence of $\nu(HSO_4)$ and $\nu'(HSO_4)$ frequencies for $[(NH_4)_{0.1}Rb_{0.9})]_3H(SO_4)_2$.

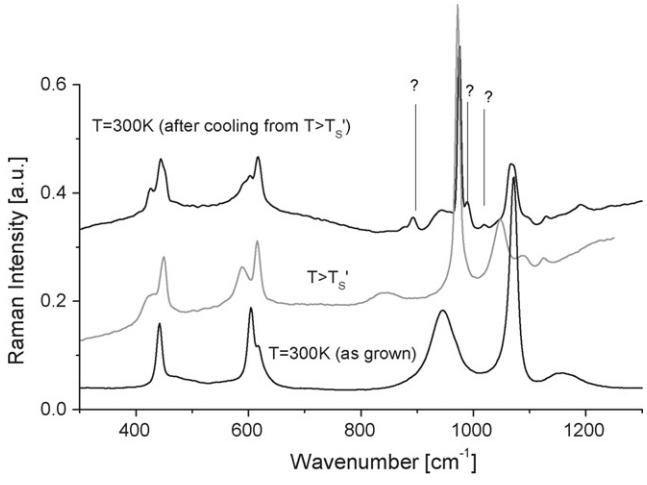

Fig. 10. Raman spectra at room temperature of crystals heated to $T > T_S'$, measured 1 day after high temperature studies.

the state where both protons in dimers and dimers themselves are ordered. Additional Raman lines, which do not exist in all phases during heating, suggest the appearance of some metastable entities, which occur while the crystal reaches the low temperature structure. These additional lines will disappear with time. Similar structural relaxation can be observed in $Rb_3H(SO_4)_2$ [16]. However, if we lower the temperature from $T_S < T < T'_S$, at room temperature we will observe a spectrum similar to the Raman spectrum of the crystal "as grown".

4. Conclusions

Our studies of $[(NH_4)_{1-x}Rb_x]_3H(SO_4)_2$ single crystals confirmed the existence of two phase transitions at T_S and T'_S with $x > 0.8$. Lower superprotonic phase (in the temperature range $T_S < T < T'_S$) by the trigonal $R\bar{3}m$ symmetry is described and the samples were in a single crystal state. The ferroelastic domain structure in the crystals under the investigation disappears at T_S. Additionally DSC and Raman studies show that if the crystal is heated to $T_S < T < T'_S$, the phase transition is reversible. Optically isotropic crystals split into blocks above T_S. At T'_S the crystal becomes polycrystalline, maintaining its macroscopic form. The transformation from phase I to phase I′ is coupled with a large change of the enthalpy. XRD studies showed that the crystal structure of phase I′ at $T > T'_S$ may be described by the Rb_2SO_4 type structure. It is very likely that due to high structural disorder in this phase we may be dealing with a gas of free protons and a durable skeleton of SO_4 groups and Rb atoms. The DSC and Raman studies revealed that the crystal which underwent a transition at T'_S, when cooled to room temperature, exhibits enormous temperature hysteresis. We can make a provisional statement that the crystals will exhibit a long-time structural relaxation, i.e. the reconstruction of both short-range (the ordering of protons in the dimer) and long-range ordering (the ordering of dimers as well as the ordering of some small micro-crystalline areas). The phase transition at T'_S in mixed crystals resembles the behavior of $Rb_3H(SO_4)_2$ crystal at its T_S. One can therefore assume that unlike the $[(NH_4)_{1-x}Rb_x]_3H(SO_4)_2$ crystals with high Rb content, which undergo a ferroelastic–paraelastic transition at T_S (I-st transition to superprotonic phase), the $Rb_3H(SO_4)_2$ crystals undergo a superprotonic phase transition only at $T = T'_S$ (see Fig. 1c).

Acknowledgment

The paper was supported by the Grant No.1P03B 03028 from the Committee of Scientific Researches in Poland.

References

[1] A.I. Baranov, I.P. Makarova, L.A. Muradyan, A.V. Tregubchenko, L.A. Shuvalov, V.I. Simonov, Sov. Phys. Crystallogr. 32 (1987) 400–407.
[2] A. Pawłowski, C. Pawlaczyk, B. Hilczer, Solid State Ionics 44 (1990) 17–19.
[3] L. Schwalowsky, U. Bismayer, Th. Lippmann, Phase Transitions 59 (1996) 61–76.
[4] Ph. Colomban, M. Pham-Thi, A. Nowak, Solid State Ionics 20 (1986) 125–134.
[5] C. Pawlaczyk, F.E. Salman, A. Pawłowski, Z. Czapla, A. Pietraszko, Phase Transitions 8 (1986) 9–16.
[6] S.M. Haile, D.A. Boysen, C.R.I. Chisholm, R.B. Merle, Nature 410 (2001) 910–913.
[7] L. Schwalowsky, V. Vinnichenko, A. Baranov, U. Bismayer, B. Merinov, G. Eckold, J. Phys.: Condens. Matter 10 (1998) 3019–3027.
[8] V.V. Sinitsyn, A.I. Baranov, E.G. Ponyatovsky, L.A. Shuvalov, Solid State Ionics 7 (1995) 118–121.
[9] K. Gesi, Phys. Status Solidi A 33 (1976) 479–482.
[10] P.M. Dominiak, J. Herold, W. Kolodziejski, K. Woźniak, Inorg. Chem. 42 (2003) 1590–1596.
[11] K. Gesi, J. Phys. Soc. Jpn. 43 (1977) 1941–1948.
[12] M. Połomska, L.F. Kirpichnikova, T. Pawłowski, B. Hilczer, Ferroelectrics 290 (2003) 51–59.
[13] A. Pawłowski, M. Połomska, Solid State Ionics 176 (2005) 2045–2051.
[14] A. Titze, J. Kusz, H. Böhm, H.-J. Weber, R. Böhmer, J. Phys.: Condens. Matter 14 (2002) 895–913.
[15] A.I. Baranov, V.V. Dolbinina, E.D. Yakushkin, V. Vinnichenko, V.H. Schmidt, S. Lanceros-Mendez, Ferroelectrics 217 (1998) 285–295.
[16] T. Pawłowski, B. Hilczer, M. Połomska, A. Pietraszko, Ferroelectrics 302 (2004) 323–325.
[17] L.F. Kirpichnikova, M. Połomska, A. Pietraszko, B. Hilczer, L. Szcześniak, Ferroelectrics 290 (2003) 61–69.
[18] M. Połomska, J. Wolak, L.F. Kirpichnikova, Ferroelectrics 334 (2006) 499–508.
[19] J. Sapriel, Phys. Rev. B 12 (1975) 5128–5140.
[20] C.J.T. Grotthus, Ann. Chim. 58 (1806) 54–73.